Ferroelectric Switchable Behavior through Fast Reversible De/adsorption of Water Spirals in a Chiral 3D Metal–Organic Framework

ARTICLE *in* JOURNAL OF THE AMERICAN CHEMICAL SOCIETY · JULY 2013

Impact Factor: 12.11 · DOI: 10.1021/ja403449k · Source: PubMed

10 AUTHORS, INCLUDING:

Bo Li
Nanjing University
400 PUBLICATIONS **3,476** CITATIONS
SEE PROFILE

li Shijun
Beijing Normal University
6 PUBLICATIONS **50** CITATIONS
SEE PROFILE

You Song
Nanjing University
234 PUBLICATIONS **6,750** CITATIONS
SEE PROFILE

Hou Wei
xi'anhangkuzhiyejishuxueyuan
535 PUBLICATIONS **8,114** CITATIONS
SEE PROFILE

JACS
JOURNAL OF THE AMERICAN CHEMICAL SOCIETY

Communication

pubs.acs.org/JACS

Ferroelectric Switchable Behavior through Fast Reversible De/adsorption of Water Spirals in a Chiral 3D Metal–Organic Framework

Xi-Yan Dong,[†] Bo Li,[†] Bin-Bin Ma,[‡] Shi-Jun Li,[†] Ming-Ming Dong,[†] Yan-Yan Zhu,[†] Shuang-Quan Zang,*[,†] You Song,*[,‡] Hong-Wei Hou,[†] and Thomas. C. W. Mak*[,†,§]

[†]College of Chemistry and Molecular Engineering, Zhengzhou University, Zhengzhou 450001, China

[‡]State Key Laboratory of Coordination Chemistry, School of Chemistry and Chemical Engineering, Nanjing National Laboratory of Microstructures, Nanjing University, Nanjing 210093, China

[§]Department of Chemistry and Center of Novel Functional Molecules, The Chinese University of Hong Kong, Shatin, New Territories, Hong Kong SAR, China

Supporting Information

ABSTRACT: A polar homochiral 3D MOF $[\{Co_2(L)(bpe)(H_2O)\}\cdot 5H_2O]_n$ constructed with cobalt(II) and a new ligand *N*-(1,3-dicarboxy-5-benzyl)-carboxymethylglycine (H_4L) accommodates ordered helical water streams in its helical grooves. It provides the first example of switchable ferroelectric and optical behavior through two-step reversible single-crystal to single-crystal transformation (SCSC) upon desorption/adsorption of water spirals and coordinated water molecules, respectively.

Metal–organic frameworks (MOFs) have potential applications in gas sorption, separation and storage, catalysis, magnetism, and optics.[1] Noncentrosymmetric and chiral MOF-based ferroelectric (FE)[2] or special dielectric[3] materials have attracted much recent interest, whereas some progress has been made with other inorganic, organic–inorganic, and organic ferroelectrics.[4] Small polar guest molecules confined in MOFs, such as water, methanol, ethanol, and organic cations often display exceptional conductivity,[5] antiferroelectric[6] or ferroelectric[7] behavior, and interesting dielectric behavior.[3] Ordered wires of hydrogen-bonded water molecules in both carbon nanotubes and nanopore membranes can exhibit spontaneous electric polarization based on molecular dynamics simulation.[8] Kobayashi's group revealed that the chain-like water clusters confined in channels of porous coordination polymer crystals showed antiferroelectric behavior at high temperature.[6a] Long et al. demonstrated that a $(H_2O)_{12n}$ wire confined within a 3D porous MOF, even in a centrosymmetric space group, can elicit a significant FE response.[9] To date, reports on ordered helical water chains confined in homochiral MOFs mainly focus on structural aspects,[10] but their electric polarity has not been extensively investigated.

In addition, single-crystal to single-crystal (SCSC) transformation accompanying drastically switchable physical property change has potential applications in molecular devices such as switches and sensors in luminescence, magnetism, and electricity.[11,12] Robust MOFs can retain their integrity when the guest molecules reversibly adsorb/desorb, thus providing a platform to directly and accurately investigate the properties of confined guest molecules or their influence on host-framework stability. However, two-step explicit fast reversible single-crystal to single-crystal (SCSC) transformation involving switchable FE and optical properties induced by desorption/adsorption of free and coordinated waters, respectively, has not been reported hitherto.

Herein, we present an unprecedented homochiral 3D MOF $[\{Co_2(L)(bpe)(H_2O)\}\cdot 5H_2O]_n$ (**1**) {H_4L = *N*-(1,3-dicarboxy-5-benzyl)carboxymethylglycine, bpe = 1,3-bis(4-pyridyl)ethene}, prepared by hydrothermal reaction of $Co(NO_3)_2\cdot 6H_2O$, H_4L, and NaOH in H_2O-MeOH. MOF **1** contains helical water columns and undergoes two-step reversible SCSC transformation concomitant with FE and optical switchable behavior upon desorption/adsorption of helical water columns and aqua ligands, respectively.

MOF **1** crystallizes in hexagonal space group $P6_1$.[13] The asymmetric unit consists of two independent Co^{2+} ions, one L, one bpe, one aqua ligand, and six free water molecules with a total site occupation factor of 5 (Supporting Information, Figure S1). Independent Co1 and Co2 ions possessing distorted octahedral geometry are bridged by two carboxylate units (O7–C13–O8 and O5–C12–O6 of carboxyl groups in bidentate mode) and one μ-O (O1) atom of another carboxylate group, resulting in a binuclear $[Co_2C_2O_5]$ motif with a Co···Co distance of 3.52 Å. Each binuclear $[Co_2C_2O_5]$ unit links four L, one aqua ligand (O1W), and two bpe to form a 6-connected node as a secondary unit. Each L serves as a μ_7-bridge to coordinate seven Co ions. A *trans*-bpe is coordinated to different Co ions through its terminal N atoms (Co1–N2 2.106 Å, Co2–N3 2.127 Å) in two binuclear $[Co_2C_2O_5]$ units (see Figures S1 and S4). The binuclear $[Co_2C_2O_5]$ motif and ligand (L) assemble two outer coaxial unequal double-helical chains designated as **A** and **B**. (Figure 1 and Figure S4). In helix **A**, the Co(II) dimers are interlinked through *m*-phenylene spacers, while they are connected by *trans*-carboxyl groups in helix **B** (Figure 1a and Figure S2a,b). Helices **A** and **B** possess the same long pitch and are interconnected by C7–N1 bonding (Figure S2c). A view down the *c*-axis easily identifies a larger hydrophilic helical channel (diameter of 16.22 Å) surrounded by host double-helical chains, with O7 (phenyl carboxylate) and O1W of helix **A** and uncoordinated O2

Received: April 10, 2013
Published: July 5, 2013

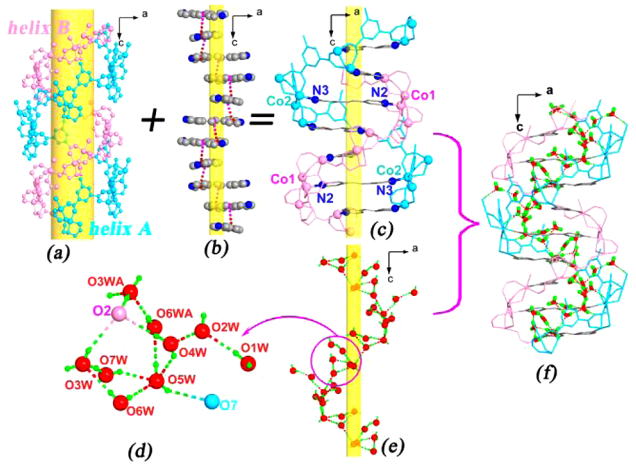

Figure 1. (a) Side view of double helix composed of unequal helix **A** and **B**, which are shown in sky blue and rose color, respectively. (b) View of helical assembly of bpe molecules. (c) View of the chiral host backbone of MOF **1**. Inner bpe (gray) molecules resemble supporting trestles that consolidate the double helix by Co−N bonds (two-colored line). (d) Hydrogen bonding interactions between water molecules and host chains; (e) View of helical water column; (f) Hydrogen-bonded helical water column in the groove of host chiral backbone of **1** (O7W′ is omitted for clarity).

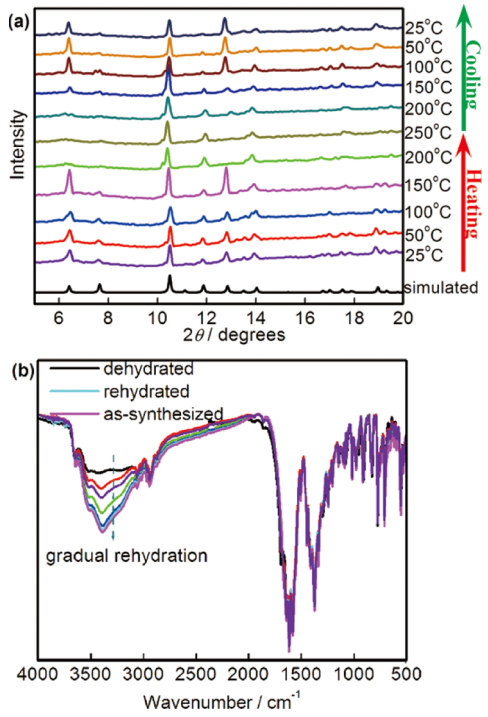

Figure 2. (a) *In situ* variable-temperature powder XRD of **1** upon both heating and cooling (25−250 °C). (b) Time-dependent IR spectra upon cooling. Color code: magenta line, as-synthesized complex **1**; black line, dehydrated phase **2**; cyan line, rehydrated form **1′**.

(iminodiacetate) of helix **B** pointing to the inner wall of the channel (Figure S2d). Moreover, binuclear $[Co_2C_2O_5]$ units extend outward to participate in construction of the adjacent helical chains. As a result, each double helix is fused to the adjacent six ones to form a 3D homochiral host framework (Figure S3). *Trans*-bpe ligands presenting the same chiral distribution apparently sustain the helical channel by Co−N bonding with helices **A** and **B** and intermolecular $\pi\cdots\pi$ interactions between adjacent bpe molecules further reinforce the structure (Figure 1c and Figure S4). Hence double-helical chains and bpe molecules cooperatively construct the chiral host rigid backbone to generate a helical groove, resulting in a helical column of water clusters intertwining the helical bpe (Figure S5).

Four lattice water molecules (O3W, O5W, O6W, O7W) assemble into a tetramer (O7W−H7WA···O3W O7W···O3W 2.72(3) Å; O7W−H7WB···O5W O7W···O5W 2.73(3) Å; O6W−H6WA···O3W O6W···O3W 2.79(0) Å; O6W−H6WB···O5W, O6W···O5W 3.25(3) Å) and the other two (O2W, O4W) suspend from O5W, which are strung together by a H-bond between O5W and O6W (O5W−H5WB···O6W, O5W···O6W 3.04(3) Å) to produce a water column (Figure 1d,e). This helical water column is further supported and stabilized by maintaining hydrogen bond networks to O1W (aqua ligand), O7 and O2 in the wall of the hydrophilic channel (O1W···O2W 2.89(9) Å, O5W···O7 2.98(0) Å and O3W···O2A 2.90(0) Å, O3W···O2B 3.27(0) Å) (Figure 1d,e and Supporting Information, Table S6). In this way, the host helical groove transfers its chirality to the helical guest water column and hence determines its orientation.

TG−DSC measurement was performed with freshly prepared crystals of **1** to determine the number of guest water molecules (n) present in the complex and to examine its thermal stability. Thermogravimetric analysis (TGA) in air revealed that the weight loss of 12.53% (calcd 12.59%) up to 150 °C and 2.47% (calcd 2.51%) between 150 and 200 °C correspond to the loss of five free and one coordinated H_2O per formula unit, respectively. The framework remains thermally stable up to 350 °C in air. Two endothermic peaks (at 108 and 170 °C) in DSC results can be attributed to the loss of free and coordinated water molecules, respectively (Figure S6).

In situ variable-temperature powder XRD (Figure 2a) showed that the powder pattern of **1** remains unchanged until 150 °C, indicating that its framework is stable after free-water removal. Some diffraction peaks disappear above 200 °C on heating, but then return at 150 °C upon cooling. No new peaks emerge and numerous major peaks maintain all along, indicating that the compound can preserve its rigid and stable framework at high temperature, and crystal-to-crystal transformation is fast and reversible. It is noted that the dehydrated phase of **1** cannot be isolated using the usual technique of high-temperature evacuation to expel solvent because its rehydration is completed within several minutes in air. Time-dependent IR spectra of an as-prepared sample of **1** show IR bands of water in the region 3600−3100 cm^{-1} (Figure S7), which nearly disappear in the dehydrated phase, but upon cooling in air they are restored to their original intensity within several minutes (Figure 2b). Other main IR bands remain unchanged, further suggesting that the host backbone is preserved before and after dehydration.

Inspired by the above results and similar reports,[14] we performed in situ variable-temperature SCXRD on **1** to explore the possibility of SCSC transformation. When single crystals of **1** were used for VT-SCXRD measurement under hot N_2 flow at 323 K, all free water molecules easily escape to give the dehydrated form $[Co_2(L)(bpe)(H_2O)]_n$ (**2**) (Figure 3b and Table S1). X-ray analysis of **2**[13] revealed that its crystal structure is virtually identical to that of **1** (a, b, c, V = 15.929, 15.929, 21.366 Å, 4694.9 $Å^3$ in **1**; and 15.883, 15.883, 21.379 Å, 4670.8 $Å^3$ in **2**).[13]

$[Co_2(L)(bpe)]_n$ (**3**) can be produced in situ at 400 K under hot N_2 flow. Crystal structure analysis showed that removal of the

dx.doi.org/10.1021/ja403449k | J. Am. Chem. Soc. 2013, 135, 10214−10217

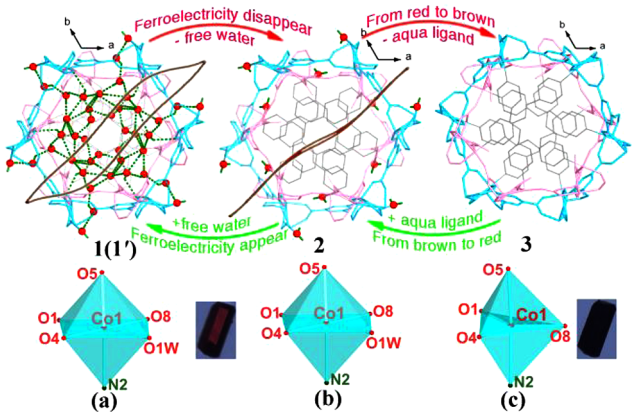

Figure 3. Schematic representation of the two-step reversible SCSC transformation between **1**, **2**, and **3** and concomitant change in structures and properties; H_2O molecules are shown as large red spheres; hydrogen bonds are indicated by green dash lines. The first step (**1**−**2**−**1′**) between structures a and b involves desorption/adsorption of free water molecules and ferroelectricity disappearing/appearing. The coordination environment of Co(II) and color of single crystal remain unchanged. The second step [**2**−**3**−(**2′**)**1′**] between structures b and c involves desorption/adsorption of aqua ligands, transformation of coordination environment of Co1 from octahedral to trigonal-bipyramidal, and color change of the single crystal from red to dark brown.

coordinated H_2O molecules causes Co1 to adopt trigonal-bipyramid coordination (Figure 3), in contrast to its octahedral environment in **1** and **2** (Figure S8 and Table S4). Accompanying this change in the Co1 coordination environment is a color change from red to dark brown (Figure 3c). However, it is noteworthy that the conformation of bpe changes dramatically to stabilize the backbone of **3** (**2**: C21−C20−C19, 127.35°; C16−C19−C20, 125.74°; N2−N3, 9.350 Å. **3**: C21−C20−C19, 115.82°; C16−C19−C20, 116.92°; N2−N3, 9.365 Å) (Figure 3 and Figure S8 and Tables S3,S4), resulting in a smaller channel along the *c* axis with a hexagonal-star cross-section. From **2** to **3**, the unit-cell volume just slightly decreases (from 4670.83 to 4632.50 $Å^3$), but the void increases appreciably (from 26.4 to 27.9%) due to the loss of aqua ligand (O1W), being consistent with the robustness of the host framework. Exposure of single crystals of **2** and **3** to moisture for a few minutes results in their reverse transformation to give the rehydrated phase **1′**[13] which is identical to **1** (Figure 3 and Table S5) and concomitant with color reversal to red (Figure 3). The reversible and repeatable optical properties of the crystal upon loss/recapture of water can be compared to thermal-induced optical switching. Both free and coordinated water molecules revert to their role in **1**, such that the length of Co1−O1W remains unchanged (**1**: Co1−O1W, 2.134(4) Å. **1′**: Co1−O1W, 2.134(5) Å) and H-bonded water spirals take on a homomorphous shape except for tiny regulation of the hydrogen bonds between guest water molecules (Figure 3, Table S6 and S7). Noteworthy is the fact that the conformation of bpe is restored to its original one (**1′**: C21−C20−C19, 128.19°; C16−C19−C20, 128.31°; N2−N3, 9.365 Å. **1**: C21−C20−C19, 126.47°; C16−C19−C20, 126.70°; N2−N3, 9.370 Å) (Figure S8). Unfortunately, the intermediate **2′** $[Co_2(L)(bpe)(H_2O)]_n$ with only coordinated O1W retrapped in the framework could not be arrested, such that guest and coordinated waters nearly revert instantly and indistinguishably into **1′** in air as soon as the hot N_2 flow is shut off (SI). The fast reversible SCSC transformations [**1**−**2**−**1′** or **1**−**2**−**3**−(**2′**)**1′**] *via* fast dehydration/rehydration processes may be attributed to robustness and hydrophilicity of the host backbone. Such two-step dehydration involving free and coordinated water and fast rehydration in SCSC is rare,[15] which may find some use in switching and sensor applications.

The most striking result in this study is ascribed to dramatic water-dependent FE switchable feature. Since a water helix is confined in the host channel of **1** (polar point group C_6) at room temperature, its FE properties were examined. Considering the crystal symmetry, the spontaneous polarization vector is parallel to the *c* axis. Single crystals of suitable size were selected to measure the dielectric hysteresis loop with electrodes made of Au wires covered by Ag-conducting glue on the approximate crystallographic (001) plane. Electric hysteresis loops were observed at room temperature under variable electric field (Figure S9). The leakage current density in the order of 10^{-8}–10^{-7} A·cm^{-2} at fields of 20 kV/cm (Figure S10) demonstrates that the observed hysteresis loops are clearly due to ferroelectricity.[2b] From the structural viewpoint, the existence of polar infinite H-bonded water columns and the spatial asymmetry may be the key factors for spontaneous polarization. However, it remains challenging to clarify the distinct origin of observed ferroelectricity in **1** owing to its very complex crystal structure. It is fortunate that **1** can undergo reversible SCSC via cyclic dehydration/rehydration and retain its polar robust network, which facilitates assessment of the contribution of the water spirals to polarization. Hence the temperature dependence of the polarization (*P*) was measured on a single crystal under an appropriate electric field (*E*) of 3.75 kV cm^{-1} parallel to the crystallographic *c*-axis (Figure 4). The hysteresis loop of as-

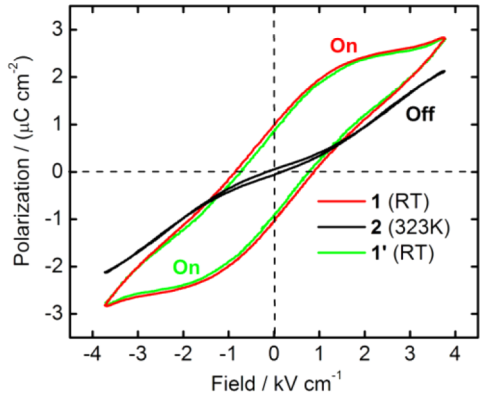

Figure 4. Hysteresis loops for the crystalline phase of **1** (as prepared at RT), **2** (dehydrated at 323K), and **1′** (rehydrated at RT) at field *(E//c)* of 3.75 kV/cm.

prepared **1** at room temperature is marked as a red line (On state). With temperature increasing to 323 K, the *P*−*E* loop shrinks to a dark loop (Off state), corresponding to the dehydrated form of **2**, which displays very small polarization induced by the chiral host backbone in the polar space group.[2,4c]

The *P*−*E* loop (green line) nearly returns to the initial state (On state, Figure 4) after exposure of **2** in moisture for a few minutes to rehydrate it to **1′**, indicating that FE polarization is almost completely restored. This reversible On/Off polarization behavior joins hands with a fast and reversible dehydration/rehydration of free water molecules (Figure 3), which can be termed "water-dependent FE switching". These experimental results demonstrated that the FE activity (On state) mainly originates from 1D H-bonded guest water columns confined in

dx.doi.org/10.1021/ja403449k | J. Am. Chem. Soc. 2013, 135, 10214−10217

the channel, which was further confirmed by QM/MM calculation (Supporting Information, section S9). The computed results indicate that the water molecules in the groove contribute more than 90% dipole moment of the *c*-axis direction of the whole model system (36 H_2O molecules included in one pitch of the helical groove). Clearly, the polarization of the water spiral is of critical importance to the inherent ferroelectricity of **1**, which is consistent with ferroelectric measurements.

Plots of the dielectric constants as a function of temperature show abroad peaks from 250 to 400 K and pronounced maxima close to 320 K (Figure 5), which may be related to changes in the

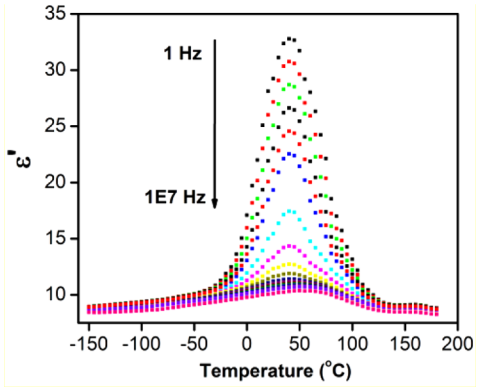

Figure 5. Temperature dependence of the dielectric constant ε' of **1** (1–10^7 Hz).

polarizability of H_2O molecules confined in the helical groove of **1**.[3a] The dielectric peak around 320 K likely indicates the disorder or gasification of water molecules and the resulting SCSC transition.[7a,16]

In summary, we report for the first time a robust chiral 3D MOF, containing infinite helical water columns, which undergoes reversible two-step SCSC transformation involving water-dependent FE and optical switching. These results point the way to probing FE properties of ordered chains of polarizable molecules or ions confined in MOFs, leading to the development of potential molecule-based multifunctional chiral materials for ferroelectrics, sensors, and switching.

■ ASSOCIATED CONTENT

Supporting Information

Experimental details, crystal structure, TGA and DSC data, crystallographic data and data collection, structure solution and refinement procedures, *P*–*E* hysteresis loop, *I*–*V* curves, and dielectric spectra, calculations for polarization, CIF data. This material is available free of charge via the Internet at http://pubs.acs.org.

■ AUTHOR INFORMATION

Corresponding Author

zangsqzg@zzu.edu.cn; yousong@nju.edu.cn; tcwmak@cuhk.edu.hk

Notes

The authors declare no competing financial interest.

■ ACKNOWLEDGMENTS

This work was supported by the National Natural Science Foundation of China (No. 20901070, No. 91022031 and No. 21021062) and Zhengzhou University.

■ REFERENCES

(1) A special issues on MOFs: (a) *Chem. Rev.* **2012**, *112*, 673–1268. (b) *Chem. Soc. Rev.* **2009**, *38*, 1201–1508.

(2) (a) Zhang, W.; Xiong, R.-G. *Chem. Rev.* **2012**, *112*, 1163–1195. (b) Sun, Z.-H.; Chen, T.-L.; Luo, J.-H.; Hong, M.-C. *Angew. Chem., Int. Ed.* **2012**, *51*, 3871–3876. (c) Pan, C.; Nan, J.-P.; Dong, X.-L.; Ren, X.-M.; Jin, W. *J. Am. Chem. Soc.* **2011**, *133*, 12330–12333.

(3) (a) Sánchez-Andújar, M.; Yáñez-Vilar, S.; Pato-Doldá, B.; Gómez-Aguirre, C.; Castro-García, S.; Señarís-Rodríguez, M. A. *J. Phys. Chem. C* **2012**, *116*, 13026–13032. (b) Cui, H.-B.; Takahashi, K.; Okano, Y.; Kobayashi, H.; Wang, Z.-M.; Kobayashi, A. *Angew. Chem., Int. Ed.* **2005**, *44*, 6508–6512.

(4) (a) Lines, M. E.; Glass, A. M. *Principles and Applications of Ferroelectrics and Related Materials*; Oxford University Press: NewYork, 1977. (b) Horiuchi, S.; Tokunaga, Y.; Giovannetti, G.; Picozzi, S.; Itoh, H.; Shimano, R.; Kumai, R.; Tokura, Y. *Nature* **2010**, *463*, 789–792. (c) Zhao, H.-R.; Li, D.-P.; Ren, X.-M.; Song, Y.; Jin, W.-Q. *J. Am. Chem. Soc.* **2010**, *132*, 18–19. (d) Nakagawa, K.; Tokoro, H.; Ohkoshi, S.-I. *Inorg. Chem.* **2008**, *47*, 10810–10812. (e) Okubo, T.; Kawajiri, R.; Mitani, T.; Shimoda, T. *J. Am. Chem. Soc.* **2005**, *127*, 17598–17599.

(5) (a) Sadakiyo, M.; Ōkawa, H.; Shigematsu, A.; Ohba, M.; Yamada, T.; Kitagawa, H. *J. Am. Chem. Soc.* **2012**, *134*, 5472–5475. (b) Sahoo, S. C.; Kundu, T.; Banerjee, R. *J. Am. Chem. Soc.* **2011**, *133*, 17950–17958. (c) Ohkoshi, S.; Nakagawa, K.; Tomono, K.; Imoto, K.; Tsunobuchi, Y.; Tokoro, H. *J. Am. Chem. Soc.* **2010**, *132*, 6620–6621.

(6) (a) Zhou, B.; Kobayashi, A.; Cui, H.-B.; Long, L.-S.; Fujimori, H.; Kobayashi, H. *J. Am. Chem. Soc.* **2011**, *133*, 5736–5739. (b) Jain, P.; Dalal, N. S.; Toby, B. H.; Kroto, H. W.; Cheetham, A. K. *J. Am. Chem. Soc.* **2008**, *130*, 10450–10451.

(7) (a) Pardo, E.; Train, C.; Liu, H.; Chamoreau, L.-M.; Dkhil, B.; Boubekeur, K.; Lloret, F.; Nakatani, K.; Tokoro, H.; Ohkoshi, S.-I.; Verdaguer, M. *Angew. Chem., Int. Ed.* **2012**, *51*, 8356–8360. (b) Yin, Y.-Y.; Chen, X.-Y.; Cao, X.-C.; Shi, W.; Cheng, P. *Chem. Commun.* **2012**, *48*, 705–707. (c) Xu, G.-C.; Ma, X.-M.; Zhang, L.; Wang, Z.-M.; Gao, S. *J. Am. Chem. Soc.* **2010**, *132*, 9588–9590. (d) Liu, C.-M.; Xiong, R.-G.; Zhang, D.-Q.; Zhu, D.-B. *J. Am. Chem. Soc.* **2010**, *132*, 4044–4045.

(8) (a) Menzl, G.; Köfinger, J.; Dellago, C. *Phys. Rev. Lett.* **2012**, *109*, 020602–1. (b) Luo, C.-F.; Fa, W.; Zhou, J.; Dong, J.-M.; Zeng, X.-C. *Nano Lett.* **2008**, *8*, 2607–2612.

(9) Zhao, H.-X.; Kong, X.-J.; Li, H.; Jin, Y.-C.; Long, L.-S.; Zeng, X.-C.; Huang, R.-B.; Zheng, L.-S. *Proc. Natl. Acad. Sci. U.S.A.* **2011**, *108*, 3481–3486.

(10) (a) Sun, X.-L.; Song, W.-C.; Zang, S.-Q.; Du, C.-X.; Hou, H.-W.; Mak, T. C. W. *Chem. Commun.* **2012**, *48*, 2113–2115. (b) Mir, M. H.; Wang, L.; Wong, M. W.; Vittal, J. J. *Chem. Commun.* **2009**, 4539–4541.

(11) (a) Kolea, G. K.; Vittal, J. J. *Chem. Soc. Rev.* **2013**, *42*, 1755–1775. (b) Vittal, J. J. *Coord. Chem. Rev.* **2007**, *251*, 1781–1795. (c) Kitagawa, S.; Matsuda, R. *Coord. Chem. Rev.* **2007**, *251*, 2490–2509.

(12) (a) Duan, C.-Y.; Wei, M.-L.; Guo, D.; He, C.; Meng, Q.-J. *J. Am. Chem. Soc.* **2010**, *132*, 3321–3330. (b) Das, M. C.; Bharadwaj, P. K. *J. Am. Chem. Soc.* **2009**, *131*, 10942–10949. (c) Bradshaw, D.; Warren, J. E.; Rosseinsky, M. J. *Science* **2007**, *315*, 977–980.

(13) For crystallographic data, see Supporting Information.

(14) (a) Wang, C.-C.; Yang, C.-C.; Yeh, C.-T.; Cheng, K.-Y.; Chang, P.-C.; Ho, M.-L.; Lee, G.-H.; Shih, W.-J.; Sheu, H.-S. *Inorg. Chem.* **2011**, *50*, 597–603. (b) Dai, F.; He, H.; Sun, D.-F. *J. Am. Chem. Soc.* **2008**, *130*, 14064–14065.

(15) (a) Cheng, X.-N.; Zhang, W.-X.; Lin, Y.-Y.; Zheng, Y.-Z.; Chen, X.-M. *Adv. Mater.* **2007**, *19*, 1494–1498. (b) Chen, C.-L.; Goforth, A. M.; Smith, M. D.; Su, C.-Y.; Loye, H.-C. *Angew. Chem., Int. Ed.* **2005**, *44*, 6673–6677.

(16) Ye, Q.; Takahashi, K.; Hoshino, N.; Kikuchi, T.; Akutagawa, T.; Noro, S.; Takeda, S.; Nakamura, T. *Chem.—Eur. J.* **2011**, *17*, 14442–14449.